

**10.3.3.2 B3GALT6**

Nakajima et al. measured the galactosyltransferase activity of *B3GALT6* in vitro using soluble-FLAG-tagged proteins for wild-type and mutant (p.Ser309Thr) which was observed common in two families and revealed the enzyme activity of the mutant protein was significantly decreased compared to the wild-type [32].

---

**10.4 D4ST1-Deficient EDS  
(MIM#601776)**

## Alternative Names

Ehlers–Danlos syndrome, type VIB, formerly  
Ehlers–Danlos syndrome, Kosho type  
Ehlers–Danlos syndrome, musculocontractural type  
Adducted thumbs, clubfoot, and progressive  
joints and skin laxity syndrome  
Adducted thumb-clubfoot syndrome (ATCS)  
Dünder syndrome  
Arthrogyposis, distal, with peculiar faces and  
hydronephrosis

**10.4.1 Clinical Manifestations**

The kyphoscoliosis type of EDS (formerly known as, EDS type VI) is characterized by generalized joint laxity, severe muscular hypotonia and scoliosis at birth, scleral fragility, and rupture of the ocular globe [2]. This disorder is essentially caused by lysyl hydroxylase deficiency (EDS type VIA); other patients with similar clinical manifestations but without lysyl hydroxylase deficiency were classified as EDS type VIB.

In 2005, Kosho et al. reported two unrelated patients with fragile and hyperextensible skin, a high propensity for bruising, generalized joint laxity, kyphoscoliosis, and the major features of EDS VI, as well as a characteristic craniofacial appearance, and multiple congenital contractures [25]. Lysyl hydroxylase deficiency was excluded in these patients by analysis of the urinary deoxypyridinoline:pyridinoline ratio, and the

patients were tentatively classified as EDS VIB. Kosho et al. subsequently reported on four additional unrelated patients and concluded that the patients represented a new type of EDS [23]. Notably, all six patients had homozygous or compound heterozygous mutations in *CHST14* [31]. Loss-of-function mutations in *CHST14* were independently found in 11 patients from four families with a rare arthrogyposis syndrome known as “adducted thumb-clubfoot syndrome (ATCS)” [9–11, 21, 43] and in three patients from two families who were originally classified as suffering from EDS VIB [27]. Malfait et al. suggested that these patients had the same disorder, which they termed “musculocontractural EDS” [27]. Shimizu et al. described the clinical characteristics of two additional patients together with a review of all of the patients reported at that time; their findings support the notion that the three independently identified conditions represent a single type of EDS [41]. Conversely, Janecke et al. claimed that the disorder should not be categorized as a type of EDS because of the presence of atypical clinical features, including facial dysmorphism, multiple congenital contractures, visceral anomalies, and impaired biosynthesis of DS as a cause of the disorder, and proposed the term DS-deficient adducted thumb-clubfoot syndrome [20]. In their response, Kosho et al. provided clinical and etiological evidence from which the disorder could be categorized as a type of EDS, because of the presence of all major features of EDS, including connective tissue fragility which required special and appropriate management of these patients. Decorin-mediated impaired assembly of collagen fibrils was the primary cause of progressive connective tissue fragility in this type [24]. Therefore, Kosho et al. proposed that the term D4ST1-deficient EDS (adducted thumb-clubfoot syndrome) was appropriate for this syndrome [24]. The current OMIM (<http://www.ncbi.nlm.nih.gov/omim>) registration of this disorder is EDS, musculocontractural type.

To date, descriptions of 26 patients (12 males, 14 females) from 17 families have been published [9–11, 21, 23, 25, 27, 30, 31, 41, 43, 46,

**Table 10.1** Classification of Ehlers-Danlos syndrome

	Prevalence/patient number	Inheritance	Causative gene
<b>Major types</b>			
Classical type	1/20,000	AD	<i>COL5A1, COL5A2</i>
Hypermobility type	1/5,000–20,000	AD	Unknown <sup>a</sup>
Vascular type	1/50,000–250,000	AD	<i>COL3A1</i>
Kyphoscoliosis type	1/100,000	AR	<i>PLOD1</i>
Arthrochalasia type	30	AD	<i>COL1A1, COL1A2</i>
Dermatosparaxis type	8	AR	<i>ADAMTS2</i>
<b>Other types</b>			
Brittle cornea syndrome	11	AR	<i>ZNF469</i>
EDS-like syndrome due to tenascin-XB deficiency	10	AR	<i>TNXB</i>
Progeroid form	7	AR	<i>B4GALT7, B3GALT6</i>
Cardiac valvular form	4	AR	<i>COL1A2</i>
EDS-like spondylocheirodysplasia	8	AR	<i>SLC39A13</i>
D4ST1-deficient EDS (DD-EDS)	22	AR	<i>CHST14</i>

AD, autosomal dominant; AR, autosomal recessive; *COL5A1*, collagen, type V, alpha 1; *COL5A2*, collagen, type V, alpha 2; *COL3A1*, collagen, type III, alpha 1; *PLOD1*, procollagen-lysine, 2-oxoglutarate 5-dioxygenase 1; *COL1A1*, collagen, type I, alpha 1; *COL1A2*, collagen, type I, alpha 2; *ADAMTS2*, ADAM metalloproteinase with thrombospondin type 1 motif, 2; *ZNF469*, zinc finger protein 469; *TNXB*, tenascin XB; *B4GALT7*, xylosylprotein beta 1,4-galactosyltransferase, polypeptide 7; *B3GALT6*, UDP-Gal:βGal β 1,3-galactosyltransferase polypeptide 6; *COL1A2*, collagen, type I, alpha 2; *SLC39A13*, solute carrier family 39 (zinc transporter), member 13; *CHST14*, carbohydrate (N-acetylgalactosamine 4-O) sulfotransferase 14

<sup>a</sup>*TNXB* mutations in a small subset of patients

48, 49]. This syndrome is characterized by a unique set of clinical features consisting of progressive systemic manifestations, including tissue fragility (e.g., skin hyperextensibility and fragility, progressive spinal and foot deformities, and large subcutaneous hematomas) and various malformations (e.g., facial features, congenital eye/heart/gastrointestinal defects, congenital multiple contractures). We have summarized the main clinical features of this syndrome in each organ in Table 10.1

#### 10.4.1.1 Craniofacial Features

The characteristic craniofacial features apparent at birth or during early infancy include a large fontanelle, hypertelorism, short and down slanting palpebral fissures, blue sclerae, a short nose with hypoplastic columella, low-set and rotated ears, a high or cleft palate, a long philtrum, a thin upper-lip vermilion, a small mouth, and micro-retrognathia (Fig. 10.4a, b). Slender and asymmetrical facial shapes with a protruding jaw are generally observed from school age onwards (Fig. 10.4c, d).

#### 10.4.1.2 Skeletal Features

Congenital multiple contractures, particularly adduction-flexion contractures of the thumbs and talipes equinovarus, are the main skeletal features (Fig. 10.4e, g, h). Fingers with a “tapering”, “slender”, and “cylindrical” shape are also common (Fig. 10.4f). Aberrant finger movement was described in three patients. Four patients had tendon abnormalities, including anomalous insertion of the flexor muscles, which probably caused the congenital contractures. Spinal deformities (e.g., scoliosis and kyphoscoliosis) and talipes deformities (e.g., planus and valgus) (Fig. 10.4i) occurred and progressed during childhood. Marfanoid habitus, recurrent joint dislocations, and pectus deformities (e.g., flat and thin, excavatum, and carinatum) were also evident. Bone mineral density was decreased in five patients and normal in two. Urine concentrations of the N-telopeptide of collagen type I, an osteoclast marker, were increased in three patients, whereas serum bone-specific alkaline phosphatase concentrations, an osteoblast marker, were normal in three, suggesting that



**Fig. 10.4** Clinical photographs of patients with D4ST1-deficient EDS. (a–d) Facial features of a patient at 23 days (a), 3 years (b), and 16 years (c, d) of age. (e, f) Images of the hand in a patient with an adducted thumb at 1 month of age (e) and cylindrical fingers at 19 years of age (f). (g–i) Images of the foot in a patient with bilateral clubfeet at 1 month of age (g, h) and progressive talipes deformities (planus and valgus) at 19 years of age (i). (j–m) Radiographs of a 16-year-old patient show diaphyseal narrowing of the

phalanges and metacarpals (j, k) and kyphoscoliosis with tall vertebral bodies (l, m). (n, o) Cutaneous features of a 19-year-old patient with hyperextensibility (n), atrophic scars, and fistula formation (o). (p) A massive cranial subcutaneous hematoma in the head of a 6-year-old patient after falling onto the floor. (q) A subcutaneous hematoma in the leg of a 16-year-old patient (All figures were originally published in Kosho et al. [23] except Fig. 10.4p, which was published in Kosho et al. [25])

increased osteoclast activity but normal osteoblast activity could cause osteopenia or osteoporosis. Radiologically, diaphyseal narrowing of the phalanges and metacarpals was noted in six patients (Fig. 10.4j, k). Talipes valgus and planus or cavum, with diaphyseal narrowing of the phalanges and metatarsals, were noted in six

patients. Tall vertebral bodies were noted in five patients (Fig. 10.4l, m).

#### 10.4.1.3 Cutaneous Features

Cutaneous features were apparent in most patients, including hyperextensibility to redundancy (Fig. 10.4n), a high propensity for bruising,

fragility leading to atrophic scars (Fig. 10.4o), acrogeria-like fine palmar creases or wrinkles, hyperalgesia to pressure, and recurrent subcutaneous infections with fistula formation. The palmar creases increased and became deeper with age.

#### 10.4.1.4 Cardiovascular Features

Large subcutaneous hematomas were common, and frequently required intensive treatment, including hospital admission, blood transfusion, and surgical drainage (Fig. 10.4p, q). The lesions were thought to be caused by the rupture of a subcutaneous artery or vein. Bleeding time was prolonged in two patients (9 min and 11 min) and was normal in three. Intranasal administration of 1-desamino-8-D-arginine vasopressin prevented the development of large subcutaneous hematomas after trauma [49]. Four patients had congenital heart defects including an atrial septal defect in three, a patent ductus arteriosus in one, and coarctation of the aorta in one. Five patients had cardiac valve abnormalities including one who underwent surgery for infectious endocarditis, which was probably caused by aortic valve or mitral valve regurgitation.

#### 10.4.1.5 Respiratory Features

Three adult patients developed pneumothorax or hemopneumothorax requiring chest tube drainage.

#### 10.4.1.6 Gastrointestinal Features

Numerous gastrointestinal abnormalities were reported, including diverticular perforation in two adult patients, constipation in seven patients, abdominal pain in two patients, and other disorders in one patient (common mesentery, absence of the gastrocolic omentum with a spontaneous volvulus of small intestine, gastric ulcer, and malrotation with duodenal obstruction).

#### 10.4.1.7 Genitourinary Features

Urological complications included nephrolithiasis or cystolithiasis in five patients, hydronephrosis in three, a dilated or atonic bladder with recurrent urinary tract infection in two, and a

horseshoe kidney in one. Cryptorchidism was observed in eight male patients, including one who underwent orchiopexy because of hypogonadism in adulthood. Poor breast development was noted in five adolescent or adult patients. No pregnant females have been reported.

#### 10.4.1.8 Ophthalmologic Features

Various ophthalmological complications have been reported, including strabismus in 12 patients, refractive errors in nine, glaucoma or elevated intraocular pressure in six, microcornea or microphthalmia in three, and retinal detachment in three.

#### 10.4.1.9 Hearing Impairment

Six patients had hearing impairments, including for high-pitched sounds in three.

#### 10.4.1.10 Growth

Patients showed mild prenatal growth retardation as the mean birth length was  $-0.5$  standard deviations (SD), the mean birth weight was  $-0.6$  SD, and the mean birth occipitofrontal circumference (OFC) was  $-0.2$  SD. Postnatal growth was also mildly impaired, as the patients were generally slender with relative macrocephaly. The mean height was  $-0.9$  SD, the mean weight was  $-1.5$  SD, and the mean OFC was  $-0.2$  SD.

#### 10.4.1.11 Development and Neuromuscular Features

Gross motor developmental delay was observed in 14 patients, as the median age of independent walking was 2 years 1 month. Two patients, aged 15 years and 32 years, could not walk unassisted. An underlying myopathic process was observed in two patients. Mild intellectual disability was apparent in four patients. One patient had a global psychomotor delay at 1.5 years of age, but his intellectual quotient was approximately 90 at the age of 7 years 2 months. Brain imaging showed ventricular enlargement and/or asymmetry in seven patients, absence of the left septum pellucidum in one patient, and a short corpus callosum, mildly prominent Sylvian fissures, and periventricular nodular heterotopias. Two patients had spinal cord tethering.

### 10.4.2 Genetic Information

Autosomal recessive inheritance was considered based on the presence of this syndrome in consanguineous families [11, 27, 31]. Three independent groups have performed homozygosity mapping and/or linkage analysis and each showed that the gene carbohydrate (*N*-acetylgalactosamine 4-*O*) sulfotransferase 14 (*CHST14*, NM\_130468.3) was responsible for this syndrome [11, 27, 31].

The *CHST14* gene was first cloned by Evers et al. [13]. It contains one coding exon (1,131-bp open reading frame) and is localized at 15q15.1. This gene encodes D4ST1, a 376 amino acid type II transmembrane protein (molecular weight: 43 kDa), that is localized in the Golgi membrane. It transfers a sulfate group from 3'-phosphoadenosine 5'-phosphosulfate to position 4 of the GalNAc residues in dermatan to generate DS (Figs. 10.1a and 10.3a). Northern blotting revealed that *CHST14* is mainly expressed in heart, placenta, liver, and pancreas, and is weakly expressed in lung, skeletal muscle, and kidney [13].

To date, 11 pathogenic mutations of *CHST14* have been identified: p.Val49\*, p.Lys69\*, p.Arg135\_Leu137delinsGlyThrGln, p.Phe209Ser, p.Arg213Pro, p.Lys226Alafs\*16, p.Arg274Pro, p.Pro281Leu, p.Cys289Ser, p.Tyr293Cys, and p.Glu334Glyfs\*107 [11, 27, 30, 31, 46, 48]. (p.Val48\* was corrected to p.Val49\*; Erratum in *Am J Med Genet Part A* 161A(2):403 (2013)) (p.Arg135Gly and p.Leu137Gln were originally reported by Dündar et al., but lately registered as c.403\_410delCGCACCCCTinsGGCACCCA, p.Arg135\_Leu137delinsGlyThrGln in The Human Gene Mutation Database: <https://portal.biobase-international.com/hgmd/pro/genesearch.php>). Because these are protein truncation mutations and missense mutations, it seems likely that the mutations cause a loss of function.

### 10.4.3 Biochemical Information

Dündar et al. reported that DS-derived IdoA-GalNAc(4S) disaccharide was undetectable in fibroblasts derived from a patient with a homozygous p.Arg213Pro mutation. They also reported

that GlcA-GalNAc(4S) content was greatly increased in the fibroblast extract and the culture media obtained from cultures of fibroblasts derived from this patient as compared with control fibroblasts [11]. It was also found that the amount of nonsulfated disaccharides (GlcA-GalNAc and IdoA-GalNAc) was increased in the cell extract and its media from the patient's fibroblast as compared with normal control fibroblasts. From these results, Dündar et al. proposed that epimerization of GlcA to IdoA by C5-carboxy epimerase is followed by sulfation of the C4 hydroxyl on the adjacent GalNAc residue by D4ST1. This process generates DS from dermatan and prevents back-epimerization from IdoA to GlcA [11, 28].

Miyake et al. measured the sulfotransferase activity of COS7 cells transfected with wild-type and mutant D4ST1 harboring the p.Lys69\*, p.Pro281Leu, p.Cys289Ser, or p.Tyr293Cys mutations. The enzyme activity of the mutants was as low as that in mock transfected cells, suggesting that these missense mutations result in the loss of function [31]. The disaccharide composition of the decorin GAG chain isolated from the patient's fibroblasts consisted only of CS, without DS, while the chains isolated from normal fibroblasts consisted of CS/DS hybrid chains [31]. Furthermore, the level of nonsulfated dermatan was negligible in the patient's fibroblasts [31]. Thus, in this syndrome, the CS/DS chain is replaced with the CS chain, even though the core proteins are normal.

### 10.4.4 Pathology and Pathophysiology

Of the major DS proteoglycans in skin, decorin was a focus of research because it binds to collagen fibrils via its core protein and its GAG chains act as interfibrillar bridges [38, 39]. Three  $\alpha$  collagen chains are self-assembled to generate tropocollagen, in the form of a triple helix. Tropocollagen then self-assembles to form collagen fibrils via decorin (Fig. 10.5a). Collagen fibrils are assembled into a collagen fiber, known as the collagen bundle, via the antiparallel com-

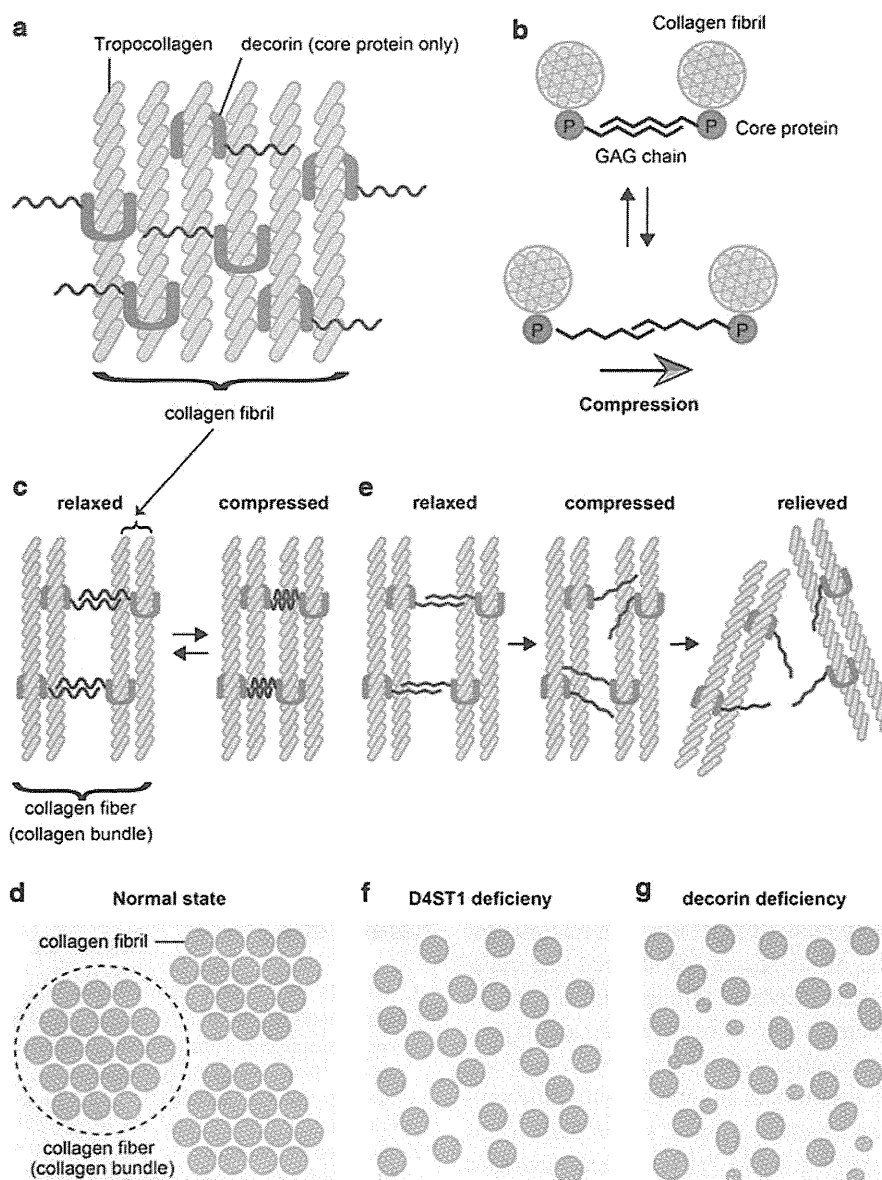


**Fig. 10.5 Putative model of abnormal collagen bundle assembly in D4ST1-deficient EDS.** (a) Tropocollagen directly binds to decorin and forms a collagen fibril. The *blue lines* represent the CS/DS hybrid chain. (b) Illustration of the sliding filament model showing reversible longitudinal slippage between the antiparallel GAG chains. The *black lines* represent unspecified GAGs. (c, d) In the normal state, the CS/DS chains can bend against the

direction of mechanical compression and rebound to the original structure (c). Thus, the collagen bundles are refractory to compression stress (d). (e, f) In D4ST1-deficient EDS, the CS/DS chains are replaced with CS chains (*red lines*). These chains cannot resist mechanical compression, resulting in irreversible scattering of the collagen fibrils. (g) The size and shape of the collagen fibrils are highly variable in decorin-deficient mice

plex of the CS/DS hybrid GAG chains of decorin, which acts like a bridge to provide a space between individual fibrils and tighten the collagen fiber (Fig. 10.5c, d).

The GAGs span collagen fibrils in the extracellular matrix of skin and tendons, and the length of the GAG chain determines the width of the interfibrillar gap [35, 36]. Elasticity of the

extracellular matrix is explained by the sliding filament model, which allows reversible longitudinal slippage between the antiparallel GAG chains (Fig. 10.5b) [39]. Because tissue stability and elasticity depend on the structure of the GAG bridges, irreversible damage can occur if the bridges are inelastic [39].

Decorin is composed of a horseshoe-shaped core protein (molecular weight: ~45 kDa) and a single CS/DS hybrid chain on the N-terminal side (Fig. 10.5a) [22, 47]. Weber et al. reported that the model structure of decorin consists of an arch in which the inner concave surface is formed from a curved  $\beta$ -sheet and the outer convex surface is formed from  $\alpha$ -helices. They also proposed that one tropocollagen fiber lies within the decorin convex and another interacts with one arm of the arch [47]. The IdoA:GlcA ratio in DS ranges from ~10 to >90 % depending on the tissue type [39]. Importantly, L-IdoA residues in DS can easily undergo conformational changes, unlike GlcA in CS [6, 7]. Thus, the IdoA:GlcA ratio should be higher in more flexible tissues [39].

Light microscopic investigation of skin specimens from two patients showed that fine collagen fibers were predominant in the reticular to papillary dermis and the number of thick collagen bundles was markedly reduced [31]. Electron microscopic examination of the specimens showed that collagen fibrils were dispersed throughout the reticular dermis, whereas they were regularly and tightly assembled in control tissue. Surprisingly, each collagen fibril was smooth and round, with little variation in size or shape, similar to the fibril in the control tissue (Fig. 10.5d, f) [31]. The disaccharide composition of the decorin GAG chain from a patient's fibroblasts only consisted of CS, without DS disaccharide, whereas control fibroblasts consisted of a CS/DS hybrid [31]. The transition of decorin from the CS/DS hybrid chain to a CS chain probably decreases the flexibility of the GAG chain. The sliding filament model proposes that mechanical compression might also work in the CS chain of D4ST1-deficient patients, but the inflexibility of the CS chain is unable to tolerate higher mechanical pressures or is too inelastic to maintain normal skin properties (Fig. 10.5e, f). This irreversible event could explain the progressive clinical course of this disease.

Interestingly, there were marked variations in the size and shape of dermal collagen fibrils in decorin-null mice (Fig. 10.5g) [8]. These findings suggest that the decorin core protein is important for collagen fibril formation, and that the CS/DS hybrid chain of decorin PG regulates the space between the collagen fibrils and form collagen bundles, as previously reported [37]. These findings suggest that the main pathological basis of this disorder could be insufficient assembly of collagen fibrils.

However, Dündar et al. reported that the light microscopic and electron microscopic findings of a patient's skin were unchanged compared to the normal control [11]. Malfait et al. reported that, in their patient, most collagen bundles were small diameter in size, and some were composed of collagen fibrils of varying diameter that were separated by irregular interfibrillar spaces [27]. In addition, the fibroblasts exhibited an elongated and/or dilated endoplasmic reticulum. So far, definitive histopathologic characteristics have not been established, so further studies are strongly encouraged to determine the major histological characteristics and underlying pathophysiology of this disorder.

---

## References

1. Almeida R, Lavery SB, Mandel U, Kresse H, Schwientek T, Bennett EP, Clausen H (1999) Cloning and expression of a proteoglycan UDP-galactose:beta-xylotriose beta1,4-galactosyltransferase I. A seventh member of the human beta4-galactosyltransferase gene family. *J Biol Chem* 274:26165–26171
2. Beighton P, De Paepe A, Steinmann B, Tsipouras P, Wenstrup RJ (1998) Ehlers-Danlos syndromes: revised nosology, Villefranche, 1997. Ehlers-Danlos National Foundation (USA) and Ehlers-Danlos Support Group (UK). *Am J Med Genet* 77:31–37
3. Bishop JR, Schuksz M, Esko JD (2007) Heparan sulphate proteoglycans fine-tune mammalian physiology. *Nature* 446:1030–1037
4. Bui C, Talhaoui I, Chabel M, Mulliert G, Coughtrie MW, Ouzzine M, Fournel-Gigleux S (2010) Molecular characterization of beta1,4-galactosyltransferase 7 genetic mutations linked to the progeroid form of Ehlers-Danlos syndrome (EDS). *FEBS Lett* 584:3962–3968
5. Bulow HE, Hobert O (2006) The molecular diversity of glycosaminoglycans shapes animal development. *Ann Rev Cell Dev Biol* 22:375–407
6. Casu B, Petitou M, Provasoli M, Sinay P (1988) Conformational flexibility: a new concept for explaining binding and biological properties of iduronic acid-

- containing glycosaminoglycans. *Trends Biochem Sci* 13:221–225
7. Catlow KR, Deakin JA, Wei Z, Delehedde M, Fernig DG, Gherardi E, Gallagher JT, Pavao MS, Lyon M (2008) Interactions of hepatocyte growth factor/scatter factor with various glycosaminoglycans reveal an important interplay between the presence of iduronate and sulfate density. *J Biol Chem* 283:5235–5248
  8. Danielson KG, Baribault H, Holmes DF, Graham H, Kadler KE, Iozzo RV (1997) Targeted disruption of decorin leads to abnormal collagen fibril morphology and skin fragility. *J Cell Biol* 136:729–743
  9. Dündar M, Demiryilmaz F, Demiryilmaz I, Kumandas S, Erkilic K, Kendirci M, Tuncel M, Ozyazgan I, Tolmie JL (1997) An autosomal recessive adducted thumb-club foot syndrome observed in Turkish cousins. *Clin Genet* 51:61–64
  10. Dündar M, Kurtoglu S, Elmas B, Demiryilmaz F, Candemir Z, Ozkul Y, Durak AC (2001) A case with adducted thumb and club foot syndrome. *Clin Dysmorphol* 10:291–293
  11. Dündar M, Müller T, Zhang Q, Pan J, Steinmann B, Vodopiutz J, Gruber R, Sonoda T, Krabichler B, Utermann G, others (2009) Loss of dermatan-4-sulfotransferase 1 function results in adducted thumb-clubfoot syndrome. *Am J Hum Genet* 85:873–882
  12. Esko JD, Kimata K, Lindahl U (2009) Proteoglycans and sulfated glycosaminoglycans. In: Varki A, Cummings RD, Esko JD, Freeze HH, Stanley P, Bertozzi CR, Hart GW, Etzler ME (eds) *Essentials of glycobiology*. Cold Spring Harbor, New York
  13. Evers MR, Xia G, Kang HG, Schachner M, Baenziger JU (2001) Molecular cloning and characterization of a dermatan-specific N-acetylgalactosamine 4-O-sulfotransferase. *J Biol Chem* 276:36344–36353
  14. Faiyaz-Ul-Haque M, Zaidi SH, Al-Ali M, Al-Mureikhi MS, Kennedy S, Al-Thani G, Tsui LC, Teebi AS (2004) A novel missense mutation in the galactosyltransferase-I (B4GALT7) gene in a family exhibiting facioskeletal anomalies and Ehlers-Danlos syndrome resembling the progeroid type. *Am J Med Genet Part A* 128A:39–45
  15. Freeze HH (2006) Genetic defects in the human glycome. *Nat Rev Genet* 7:537–551
  16. Hernandez A, Aguirre-Negrete MG, Gonzalez-Flores S, Reynoso-Luna MC, Fragoso R, Nazara Z, Tapia-Arizmendi G, Cantu JM (1986) Ehlers-Danlos features with progeroid facies and mild mental retardation. Further delineation of the syndrome. *Clin Genet* 30:456–461
  17. Hernandez A, Aguirre-Negrete MG, Liparoli JC, Cantu JM (1981) Third case of a distinct variant of the Ehlers-Danlos Syndrome (EDS). *Clin Genet* 20:222–224
  18. Hernandez A, Aguirre-Negrete MG, Ramirez-Soltero S, Gonzalez-Mendoza A, Martinez y Martinez R, Velazquez-Cabrera A, Cantu JM (1979) A distinct variant of the Ehlers-Danlos syndrome. *Clin Genet* 16:335–339
  19. Jaeken J, Hennet T, Freeze HH, Matthijs G (2008) On the nomenclature of congenital disorders of glycosylation (CDG). *J Inher Metab Dis* 31:669–672
  20. Janecke AR, Baenziger JU, Müller T, Dündar M (2011) Loss of dermatan-4-sulfotransferase 1 (D4ST1/CHST14) function represents the first dermatan sulfate biosynthesis defect, “dermatan sulfate-deficient adducted thumb-club-foot syndrome”. *Hum Mutat* 32:484–485
  21. Janecke AR, Unsinn K, Kreczy A, Baldissera I, Gassner I, Neu N, Utermann G, Müller T (2001) Adducted thumb-club foot syndrome in sibs of a consanguineous Austrian family. *J Med Genet* 38:265–269
  22. Kobe B, Deisenhofer J (1993) Crystal structure of porcine ribonuclease inhibitor, a protein with leucine-rich repeats. *Nature* 366:751–756
  23. Kosho T, Miyake N, Hatamochi A, Takahashi J, Kato H, Miyahara T, Igawa Y, Yasui H, Ishida T, Ono K, others (2010) A new Ehlers-Danlos syndrome with craniofacial characteristics, multiple congenital contractures, progressive joint and skin laxity, and multi-system fragility-related manifestations. *Am J Med Genet Part A* 152A:1333–1346
  24. Kosho T, Miyake N, Mizumoto S, Hatamochi A, Fukushima Y, Yamada S, Sugahara K, Matsumoto N (2011) A response to: loss of dermatan-4-sulfotransferase 1 (D4ST1/CHST14) function represents the first dermatan sulfate biosynthesis defect, “dermatan sulfate-deficient Adducted Thumb-Clubfoot Syndrome”. Which name is appropriate, “Adducted Thumb-Clubfoot Syndrome” or “Ehlers-Danlos syndrome”? *Hum Mutat* 32:1507–1509
  25. Kosho T, Takahashi J, Ohashi H, Nishimura G, Kato H, Fukushima Y (2005) Ehlers-Danlos syndrome type VIB with characteristic facies, decreased curvatures of the spinal column, and joint contractures in two unrelated girls. *Am J Med Genet Part A* 138A:282–287
  26. Kresse H, Rosthoj S, Quentin E, Hollmann J, Glossl J, Okada S, Tonnesen T (1987) Glycosaminoglycan-free small proteoglycan core protein is secreted by fibroblasts from a patient with a syndrome resembling progeroid. *Am J Hum Genet* 41:436–453
  27. Malfait F, Syx D, Vlummens P, Symoens S, Nampoothiri S, Hermanns-Le T, Van Laer L, De Paepe A (2010) Musculocontractural Ehlers-Danlos Syndrome (former EDS type VIB) and adducted thumb clubfoot syndrome (ATCS) represent a single clinical entity caused by mutations in the dermatan-4-sulfotransferase 1 encoding CHST14 gene. *Hum Mutat* 31:1233–1239
  28. Malmström A (1984) Biosynthesis of dermatan sulfate. II. Substrate specificity of the C-5 uronosyl epimerase. *J Biol Chem* 259:161–165
  29. Mao JR, Bristow J (2001) The Ehlers-Danlos syndrome: on beyond collagens. *J Clin Invest* 107:1063–1069
  30. Mendoza-Londono R, Chitayat D, Kahr WH, Hinek A, Blaser S, Dupuis L, Goh E, Badilla-Porras R, Howard A, Mittaz L, others (2012) Extracellular matrix and platelet function in patients with musculo-



- contractural Ehlers-Danlos syndrome caused by mutations in the CHST14 gene. *Am J Med Genet Part A* 158A:1344–1354
31. Miyake N, Kosho T, Mizumoto S, Furuichi T, Hatamochi A, Nagashima Y, Arai E, Takahashi K, Kawamura R, Wakui K, others (2010) Loss-of-function mutations of CHST14 in a new type of Ehlers-Danlos syndrome. *Hum Mutat* 31:966–974
  32. Nakajima M, Mizumoto S, Miyake N, Kogawa R, Iida A, Ito H, Kitoh H, Hirayama A, Mitsubuchi H, Miyazaki O, others (2013) Mutations in B3GALT6, which encodes a glycosaminoglycan linker region enzyme, cause a spectrum of skeletal and connective tissue disorders. *Am J Hum Genet* 92:927–934
  33. Okajima T, Fukumoto S, Furukawa K, Urano T (1999) Molecular basis for the progeroid variant of Ehlers-Danlos syndrome. Identification and characterization of two mutations in galactosyltransferase I gene. *J Biol Chem* 274:28841–28844
  34. Okajima T, Yoshida K, Kondo T, Furukawa K (1999) Human homolog of *Caenorhabditis elegans* sqv-3 gene is galactosyltransferase I involved in the biosynthesis of the glycosaminoglycan-protein linkage region of proteoglycans. *J Biol Chem* 274:22915–22918
  35. Scott JE (1988) Proteoglycan-fibrillar collagen interactions. *Biochem J* 252:313–323
  36. Scott JE (1992) Morphometry of cupromeronic blue-stained proteoglycan molecules in animal corneas, versus that of purified proteoglycans stained in vitro, implies that tertiary structures contribute to corneal ultrastructure. *J Anat* 180(Pt 1):155–164
  37. Scott JE (1995) Extracellular matrix, supramolecular organisation and shape. *J Anat* 187(Pt 2):259–269
  38. Scott JE (1996) Proteodermatan and proteokeratan sulfate (decorin, lumican/fibromodulin) proteins are horseshoe shaped. Implications for their interactions with collagen. *Biochemistry* 35:8795–8799
  39. Scott JE (2003) Elasticity in extracellular matrix ‘shape modules’ of tendon, cartilage, etc. A sliding proteoglycan-filament model. *J Physiol* 553:335–343
  40. Seidler DG, Faiyaz-Ul-Haque M, Hansen U, Yip GW, Zaidi SH, Teebi AS, Kiesel L, Gotte M (2006) Defective glycosylation of decorin and biglycan, altered collagen structure, and abnormal phenotype of the skin fibroblasts of an Ehlers-Danlos syndrome patient carrying the novel Arg270Cys substitution in galactosyltransferase I (beta4GalT-7). *J Mol Med (Berl)* 84:583–594
  41. Shimizu K, Okamoto N, Miyake N, Taira K, Sato Y, Matsuda K, Akimaru N, Ohashi H, Wakui K, Fukushima Y, others (2011) Delineation of dermatan 4-O-sulfotransferase 1 deficient Ehlers-Danlos syndrome: observation of two additional patients and comprehensive review of 20 reported patients. *Am J Med Genet Part A* 155A:1949–1958
  42. Sisu E, Flangea C, Serb A, Zamfir AD (2011) Modern developments in mass spectrometry of chondroitin and dermatan sulfate glycosaminoglycans. *Amino Acids* 41:235–256
  43. Sonoda T, Kouno K (2000) Two brothers with distal arthrogyrosis, peculiar facial appearance, cleft palate, short stature, hydronephrosis, retentio testis, and normal intelligence: a new type of distal arthrogyrosis? *Am J Med Genet* 91:280–285
  44. Steinmann B, Royce PM, Superti-Furga A (2002) The Ehlers-Danlos syndrome. In: Royce PM and Steinmann B (eds) *Connective tissue and its heritable disorders*. (2nd edition) Wiley-Liss, Inc., New York
  45. Sugahara K, Mikami T, Uyama T, Mizuguchi S, Nomura K, Kitagawa H (2003) Recent advances in the structural biology of chondroitin sulfate and dermatan sulfate. *Curr Opin Struct Biol* 13:612–620
  46. Voermans NC, Kempers M, Lammens M, van Alfen N, Janssen MC, Bonnemann C, van Engelen BG, Hamel BC (2012) Myopathy in a 20-year-old female patient with D4ST-1 deficient Ehlers-Danlos syndrome due to a homozygous CHST14 mutation. *Am J Med Genet Part A* 158A:850–855
  47. Weber IT, Harrison RW, Iozzo RV (1996) Model structure of decorin and implications for collagen fibrillogenesis. *J Biol Chem* 271:31767–31770
  48. Winters KA, Jiang Z, Xu W, Li S, Ammous Z, Jayakar P, Wierenga KJ (2012) Re-assigned diagnosis of D4ST1-deficient Ehlers-Danlos syndrome (adducted thumb-clubfoot syndrome) after initial diagnosis of Marden-Walker syndrome. *Am J Med Genet A* 158A:2935–2940
  49. Yasui H, Adachi Y, Minami T, Ishida T, Kato Y, Imai K (2003) Combination therapy of DDAVP and conjugated estrogens for a recurrent large subcutaneous hematoma in Ehlers-Danlos syndrome. *Am J Hematol* 72:71–72

## Haploinsufficiency of *STXBP1* and Ohtahara syndrome

Hiroto Saito<sup>1</sup>

Mitsuhiro Kato<sup>2</sup>

Naomichi Matsumoto<sup>1</sup>

<sup>1</sup> Department of Human Genetics, Yokohama City University Graduate School of Medicine

<sup>2</sup> Department of Pediatrics, Yamagata University Faculty of Medicine

### Abstract

Ohtahara syndrome (OS) is one of the most severe and earliest forms of epilepsy. Brain malformations or metabolic disorders are often associated with OS, but other cases remain etiologically unexplained. Here we show that *de novo* heterozygous mutations in the gene encoding *STXBP1*, also known as *MUNC18-1*, which is essential in synaptic vesicle release in multiple species, cause OS. A microdeletion involving *STXBP1* and various point mutations, including missense, frameshift, nonsense, and splicing mutations, have been found in individuals with OS. Transcripts associated with frameshift, nonsense, and splicing mutations are likely to be degraded by nonsense mediated mRNA decay. Moreover, *STXBP1* proteins harboring missense mutations were unstable compared with the wild-type, and were degraded in Neuroblastoma2A cells. Binding of a mutant protein (p.C180Y) to syntaxin-1A was also significantly impaired. These findings strongly suggest that haploinsufficiency of *STXBP1* causes OS. Mutations of *STXBP1* also suggest that aberrations of genes involved in synaptic vesicle release might be associated with other types of infantile epilepsy.

### Brief introduction

Ohtahara syndrome (OS), also known as early infantile epileptic encephalopathy with suppression-burst, is one of the most severe and earliest forms of epilepsy.<sup>1</sup> It is characterized by early onset of tonic seizures, seizure intractability, characteristic suppression-burst patterns on the electroencephalogram (EEG), and a poor outcome with severe psychomotor retardation.<sup>2,3</sup> Brain malformations, such as cerebral dysgenesis or hemimegalencephaly, are often associated with OS, but cryptogenic or idiopathic OS is found in a subset of OS patients, in whom genetic aberrations might be involved.<sup>4</sup> Although mutations of the *ARX* gene have been found in several male patients with OS,<sup>5-8</sup> the genetic causes are unexplained in most cryptogenic OS cases. We have recently found *de novo* mutations in *STXBP1* (encoding syntaxin binding protein 1, also known as *MUNC18-1*) in individuals with cryptogenic OS.<sup>9</sup> Here we present all the mutations in *STXBP1* found to date in OS patients, as well as some evidence of mutations leading to haploinsufficiency.

### OHTAHARA SYNDROME

Ohtahara syndrome was first reported as the earliest form of age-dependent epileptic syndromes by Ohtahara et al.<sup>1</sup> It is characterized by early onset of intractable tonic spasms, characteristic suppression-burst patterns on interictal EEG, and a poor outcome with severe psychomotor retardation.<sup>2,3</sup> According to a previous report,<sup>4</sup> all patients have seizure onset

Address correspondence to: Dr. Hiroto Saito, Department of Human Genetics, Yokohama City University Graduate School of Medicine, 3-9 Fukuura, Kanazawa-ku, Yokohama 236-0004, Japan. Tel.: +81-45-787-2606, Fax: +81-45-786-5219, E-mail: hsaito@yokohama-cu.ac.jp.

within the first 3 months, with the majority (75%) in the first month. Tonic spasms were observed in all patients. One-third to one-half of patients also had partial seizures, such as erratic focal motor seizures and hemiconvulsions, or asymmetric tonic seizures; however, myoclonic seizures were rare. Hemiconvulsions, tonic seizures, or clonic seizures precede the onset of tonic spasms by 1 to several weeks to in 37.5% of OS patients.<sup>4</sup> Brain malformations, such as cerebral dysgenesis, hemimegalencephaly, porencephaly, and Aicardi syndrome are often associated with OS, but a significant proportion of patients (31% to 50% of OS cases) remain etiologically unexplained.<sup>2,4</sup> Suppression-burst patterns on interictal EEG consisting of high-voltage activity alternating with nearly flat suppression phases are observed when the patient is both awake and asleep.

Early myoclonic encephalopathy (EME) is another epileptic syndrome showing suppression-burst patterns on EEG.<sup>10</sup> The prevailing initial seizure type is a main difference between OS and EME: tonic seizures in OS and myoclonic seizures in EME.<sup>2,3</sup> However, OS and EME have common features, and it is often difficult to distinguish between them. Homozygous missense mutations of the *SLC25A22* (mitochondrial glutamate carrier 1) gene have been recently found in EME individuals in consanguineous families.<sup>11,12</sup> Age-dependent evolution is a characteristic feature of both OS and EME: approximately 75% and 40% of OS and EME cases transit to West syndrome (WS) usually 3–4 months afterwards.<sup>2,3</sup> West syndrome is characterized by tonic spasms with clustering, arrest of psychomotor development, and hypsarrhythmia on EEG. Such transitions suggest a common pathophysiology between OS and WS or between EME and WS. Consistent with this hypothesis, specific mutations of the *ARX* (*aristaless*-related homeobox) gene at Xp22.13, have been recently found in male OS and WS cases.<sup>5–8,13–15</sup>

## DE NOVO STXBP1 MUTATIONS CAUSE OS

### Identification of *STXBP1* Mutations in Patients with OS

Through BAC array-based comparative genomic hybridization analysis of patients associated with mental retardation (MR), we found a microdeletion at 9q33.3-q34.11 in a female patient with OS.<sup>9</sup> As the microdeletion occurred *de novo*, we assumed that a gene within the deletion was responsible for OS. Among the genes mapped within the deletion, the gene encoding syntaxin binding protein 1 (*STXBP1*) was of particular interest because mouse *Stxbp1* has been shown to be essential for synaptic vesicle release<sup>16</sup> and is specifically expressed in the brains of rodents and humans.<sup>17,18</sup> We therefore analyzed *STXBP1* in 13 unrelated patients with OS. Four heterozygous missense mutations were found at evolutionary conserved amino acids in three males and one female (Figure 1 and Table 1). Three mutations were confirmed as *de novo* events (paternal DNA was unavailable for one remaining mutation).

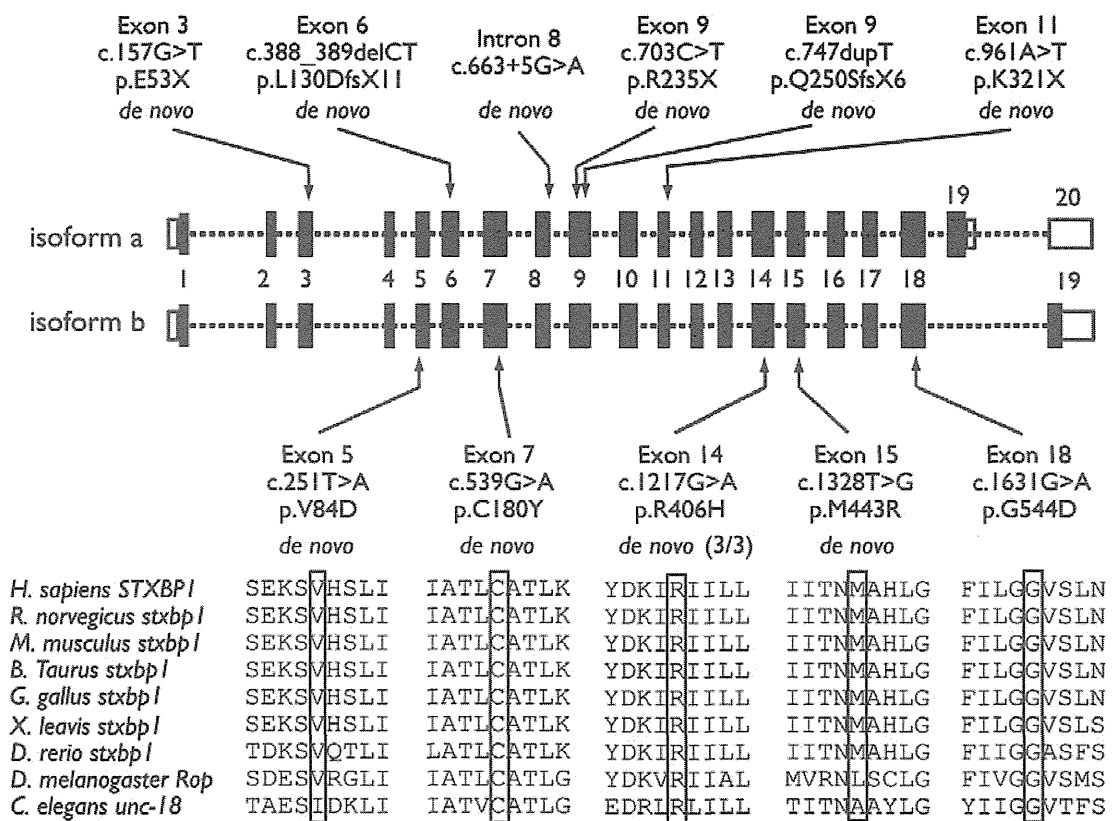


**Figure 1. Summary of *STXBPI* mutations found in Japanese individuals with OS**

Schematic representation of *STXBPI*, consisting of at most 20 exons (the UTR and the coding region are open and filled rectangles, respectively). There are two isoforms, a (GenBank accession number, NM\_003165) with exon 19, and b (NM\_001032221) without exon 19 of isoform a. Locations of mutations are indicated by arrows. Eleven different mutations are presented: missense mutations are indicated below the gene scheme, and the other types of mutations are indicated above the gene. Ten mutations in 12 subjects occurred *de novo*. All missense mutations occurred at conserved amino acids. CLUSTALW (<http://align.genome.jp/>) was used to align homologs of different species. Adapted from Refs.<sup>9</sup> and <sup>19</sup>

**Table 1**  
**Summary of Clinical Features of Subjects with *STXBP1* Deletion/Mutations**

Case # Mutation	Initial Symptoms	Onset of Spasms	Transition from Spasms to Other Seizures	Response to Therapy
#1 Deletion	Tonic seizure and oral automatism	2 m	Generalized clonic seizure at 29 m	Seizure free from 5m after TRH injection
#2 c.1631G>A	Blinking	10 d	No	Seizure free from 3m
#3 c.539G>A	Tonic seizure with blinking	3 m	No	Intractable, daily
#4 c.1328T>G	Upward gazing and tonic seizure	2 m	Partial seizure at 8 m	Intractable, hourly TRH injection was temporally effective
#5 c.251T>A	Spasms and tonic-clonic seizure	2 m	No	Intractable, daily
#6 c.1217G>A	Generalized convulsions	3 w	No	Intractable, hourly
#7 c.1217G>A	GTCS with upward eye gazing	2 m	Myoclonic seizure at 48 d	Intractable, daily
#8 .1217G>A	Partial seizures (right hemi convulsion)	2 m	Tonic seizure to myoclonic seizure	Intractable, daily
#9 c.157G>T	Spasms	2 d	Versive seizure after hypoxia at 2 y	Intractable, daily
#10 c.388_389del	Secondary generalized seizures	2 m	CPS	Seizure free after ACTH or VPA with KBr
#11 c.663+5G>A	Blinking to tonic seizures	1 m	Tonic seizure	Seizure free with VB6 for spasms and ACTH for WS
#12 c.703C>T	Spasms in cluster	1 m	No	Seizure free from 6 m after high-dose PB
#13 c.747dup	Clonic convulsion	31 d	Partial seizure and myoclonic seizures	Intractable, hourly
#14 c.961A>T	Partial seizures	3 w	Partial seizure	Intractable, daily

GTCS, generalized tonic-clonic seizures; CPS, complex partial seizure; TRH, thyrotropin-releasing hormone; ACTH, adrenocorticotropic hormone; VPA, valproic acid; KBr, Potassium bromide; VB6, vitamin B6; PB, phenobarbital; d, day(s); w, week; m, month(s); y, year(s); 0 w, 0 to 6 days; 0 m, 0 to 3 weeks

### ***STXBP1* Mutation Is a Major Genetic Cause of OS**

To delineate the clinical spectrum of patients with *STXBP1* mutations, *STXBP1* was further analyzed in 29 and 54 cases of cryptogenic OS and WS, respectively.<sup>19</sup> No brain malformations were found in any of the cases. Seven novel heterozygous mutations were found in nine OS cases (the same mutation was found in three cases), but none in WS cases (six males and three females: Figure 1 and Table 1). The mutations included one missense, one splicing, two frameshift, and three nonsense mutations. A recurrent missense mutation (c.1217G>A, p.R406H) occurred at an evolutionarily conserved amino acid (Figure 1). All the mutations occurred *de novo*. Collectively, *STXBP1* aberrations account for about one-third of individuals

with OS (14 out of 43). These data showed that *STXBP1* mutations are a major genetic cause of cryptogenic OS, but they are not a genetic cause of WS in our Japanese cohort.

### Clinical Features of Patients with *STXBP1* Deletion/Mutations

Clinical information from 14 individuals with confirmed *STXBP1* deletion/mutations is summarized in Table 1. These persons showed distinctive features of OS, such as early-onset seizures including epileptic spasms, suppression-burst pattern on EEG, transition to WS after a few to several months, and severe developmental delay. Epileptic spasms were preceded by other seizure types, including partial seizures in 11 subjects. Transition to WS was observed in 11 subjects with OS. Although seizures were intractable in nine subjects, five subjects responded to medication, such as thyrotropin-releasing hormone (TRH) injection, adrenocorticotrophic hormone (ACTH) injection, vitamin B<sub>6</sub>, high-dose phenobarbital, and valproic acid. All subjects demonstrated severe psychomotor developmental delay. Brain magnetic resonance imaging (MRI) showed no structural anomalies or hippocampal anomalies but did show some atrophy (Figure 2A). Suppression-burst on interictal EEG was observed in both awake and asleep states (Figure 2B). We gained several insights into the phenotype of *STXBP1* aberrations. Firstly, the age at onset of epileptic spasms is later in subjects with *STXBP1* aberrations than in the 16 original subjects reported by Yamatogi and Ohtahara.<sup>4</sup> Only 27 % of the subjects (4/15) in our series had onset of OS within 1 month compared to 75 % (12/16) in the series of Yamatogi and Ohtahara. As subjects with *STXBP1* aberrations showed no structural anomalies on brain MRI examination, the onset of epileptic seizures might be affected by associated structural brain abnormalities, which are commonly seen in other reports of OS. Secondly, myoclonic seizures, which are thought to be rarely observed in OS, were occasionally observed (3/14). Myoclonic seizures are the main ictal symptom of EME. These three subjects can be diagnosed as having EME when myoclonic seizures dominate. Thus, *STXBP1* might also be causative for EME, implying a genetic linkage between OS and EME. Another infrequent but interesting finding is that one patient (no.5) developed vigorous chorea-ballismus subsequent to OS, suggesting that mutations of *STXBP1* could affect the basal ganglia.<sup>9,20</sup> In terms of the genotype-phenotype relationship, we found no difference in clinical data between seven subjects with missense mutations and seven subjects with microdeletions, premature termination codons, or splicing mutations. This finding is supported by our experimental data that demonstrated both missense mutations and a splicing mutation resulted in haploinsufficiency of *STXBP1*: degradation of STXBP1 proteins containing missense mutations and nonsense-mediated mRNA decay (NMD) associated with aberrantly spliced mRNAs (see below).

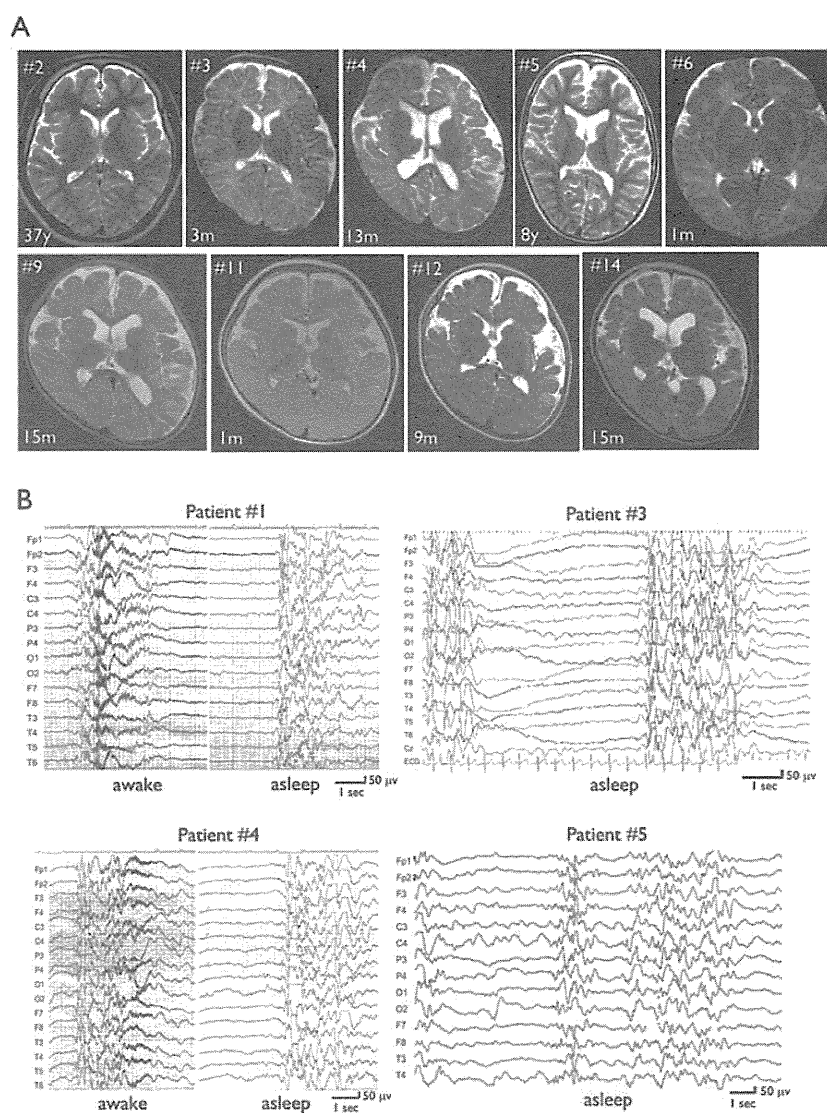


**Figure 2. Brain MRI scan and EEG of OS patients with *STXBP1* aberrations**  
 (A) Brain MRI (T2-weighted axial) image through the basal ganglia shows normal brain structure in patients with *STXBP1* mutations. Patient IDs and developmental stages are indicated. Mild dilatation of lateral ventricles is observed in patients #4, #9, #11, and #14, but none shows brain malformation. y, year(s); m, month(s). (B) Suppression-burst on interictal EEG of patients #1 (at age 2 months), #3 (at 3 months), #4 (at 2 months), and #5 (at 3 months). High-voltage bursts alternating with almost flat suppression phases at an approximately regular rate in both awake and asleep states. Adapted from Refs.<sup>9</sup> and <sup>19</sup>

## MOLECULAR EVIDENCE OF *STXBP1* HAPLOINSUFFICIENCY

### Mutant *STXBP1* Proteins Are Unstable

All five missense mutations lead to amino acid replacements in the hydrophobic core of *STXBP1* and are considered to destabilize the folding architecture. This is especially true for the three mutants (p.V84D, p.G544D and p.M443R) that have replaced the wild-type (WT) residues with charged residues, which would be predicted to severely disrupt the conformation of *STXBP1*.<sup>9</sup> In fact, circular dichroism (CD) spectra showed that the helical content of the C180Y mutant is lower (39%) than that of the WT (43%), suggesting that the mutation

destabilized the secondary structure of STXBP1<sup>9</sup> (Figure 3A). Moreover, CD melting experiments revealed that the melting temperature ( $T_m$ ) of the C180Y mutant was about 11 degrees lower than that of the WT (Figure 3B), indicating that the C180Y mutant is much more unstable than the WT. The regulation of synaptic vesicle release by Stxbp1 is mediated in part by binding to Syntaxin-1A as well as directly to the Soluble N-ethylmaleimide-sensitive factor attachment protein receptor (SNARE) complex, which mediates fusion of vesicles with the target membrane.<sup>21,22</sup> Binding of a mutant protein (p.C180Y) to syntaxin-1A was also significantly impaired, even at 4 °C in vitro.<sup>9</sup> Together with the fact that the  $T_m$  of the C180Y mutant is close to the physiological temperature of the human body, it is less likely that its functional activity could be retained in the human brain. Other STXBP1 mutants (p.V84D, p.G544D, and p.M443R) tend to form aggregates, and thus sufficient protein for biophysical analyses could not be obtained.

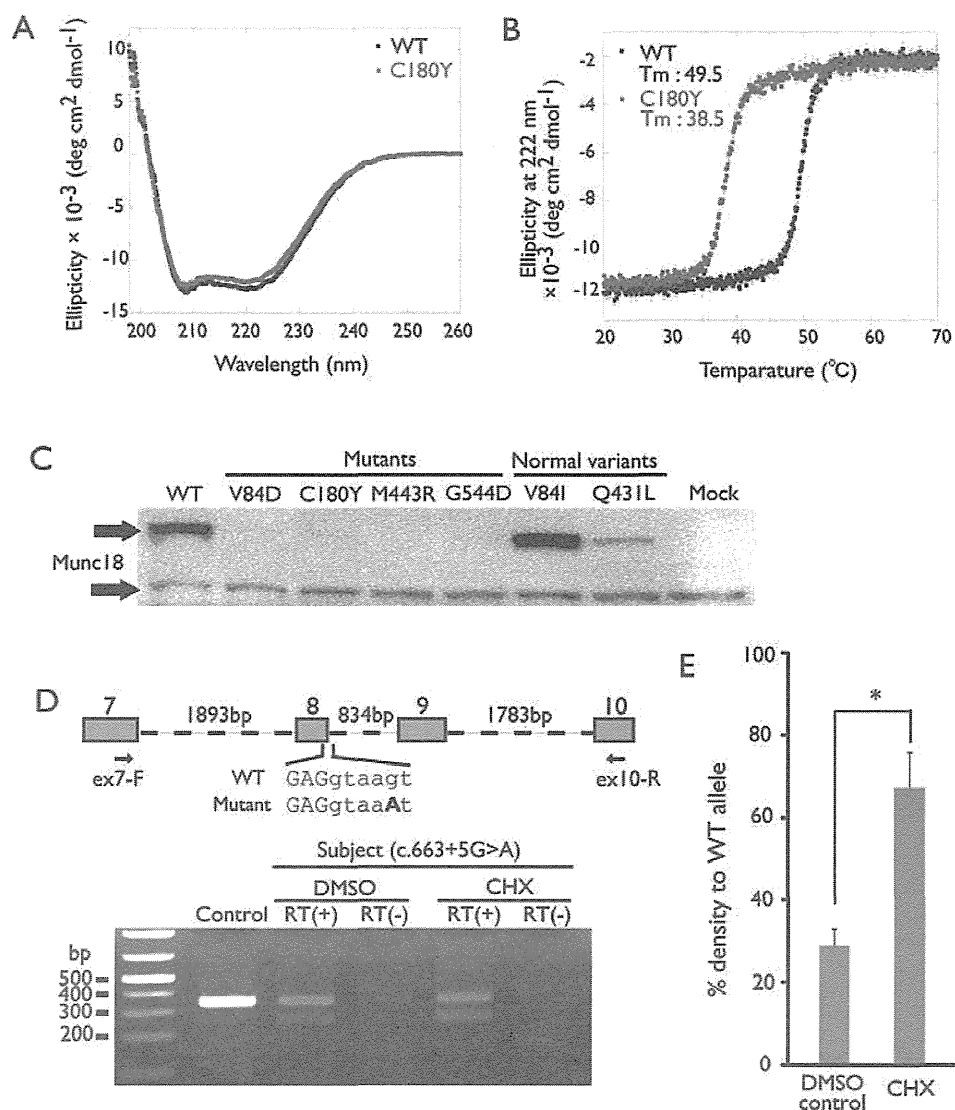


**Figure 3. Characterization of mutant STXBP1 proteins and mRNAs with aberrant splicing**  
 (A) Circular dichroism spectra of the WT and C180Y-mutated STXBP1. The C180Y mutation is found to induce a subtle decrease in the helical contents of the STXBP1 structure by comparing the peaks of both proteins at 222 nm, where a large negative ellipticity



value indicates a high helical content of the protein. (B) Circular dichroic melting curves of the STXBP1 WT and C180Y proteins. Values of ellipticity at 222 nm are measured to monitor the thermal unfolding of the proteins. The C180Y mutant became unfolded at a lower temperature compared to the WT. Each dot represents the average of three repeated experiments, with standard deviations depicted as error bars. (C) Immunoblot analysis of mutant STXBP1 proteins using a monoclonal anti-Munc18 antibody. Upper and lower bands represent EGFP-STXBP1 and endogenous STXBP1 proteins, respectively. Expression of four mutant STXBP1 proteins was not detected, while the WT and two normal variants could be detected. (D) (Top) Schematic representation of the genomic structure from exons 7 to 10 of *STXBP1*. Exons, introns, and primers are shown by boxes, dashed lines, and arrows, respectively. Sequences of exons and introns are presented in uppercase and lower-case, respectively. The mutation in intron 8 is highlighted in bold. (Bottom) Reverse transcriptase-PCR analysis of patient #11 with a c.663+5G>A mutation and a normal control. Two PCR products were detected from the patient's cDNA: the upper one is the WT transcript and the lower one is the mutant. Only a single WT amplicon was detected in the control. The mutant amplicon was significantly increased by 30  $\mu$ M cycloheximide (CHX) treatment compared to dimethyl sulfoxide (DMSO) treatment as a vehicle control. RT (+): with reverse transcriptase, RT (-): without reverse transcriptase as a negative control. (E) Quantitative analysis of the NMD inhibition by CHX based on the data shown in (D). \* $P = 0.0023$  by unpaired Student's *t*-test, two tailed. Averages of three repeated experiments are shown with error bars (s.d). Adapted from Refs. <sup>9</sup> and <sup>19</sup>

### Degradation of Mutant STXBP1 Proteins

Transient expression of mutant STXBP1 proteins in Neuroblastoma 2A (N2A) cells showed further evidence of *STXBP1* haploinsufficiency. The WT EGFP-STXBP1 was expressed in the cytosolic compartment, but not in the nucleus or plasma membrane, similar to endogenous expression.<sup>9,23</sup> However, in approximately 20% of cells expressing mutant EGFP-STXBP1 (p.V84D, p.C180Y, p.M443R, and p.G544D), intense clusters of fluorescence signals were observed, likely representing protein aggregation.<sup>9</sup> The other 80% of cells showed a diffuse cytosolic protein distribution similar to that expressing the WT, but the signal intensity was much weaker, implying possible protein degradation. Protein degradation of mutant STXBP1 proteins was also confirmed by immunoblotting using an anti-Munc18 antibody<sup>19</sup> (Figure 3C). These experiments suggested that mutant STXBP1 proteins would be aggregated or degraded in neurons, both leading to loss of STXBP1 function.

### Degradation of *STXBP1* mRNA with Abnormal Splicing

The splicing, frameshift, and nonsense mutations would produce a premature stop codon; therefore, these mutant mRNAs are likely to be degraded by NMD.<sup>24,25</sup> In fact, NMD associated with abnormal splicing was demonstrated in lymphoblastoid cells derived from a patient harboring a c.663+5G>A mutation. Polymerase chain reaction (PCR) primers designed to amplify exons 7 to 10 amplified a single band (338 bp), corresponding to the WT *STXBP1* allele, using a cDNA template from a control lymphoblastoid cell lines (LCL; Figure 3D). By contrast, a smaller band was detected from the patient's cDNA, in which exon 8 of *STXBP1* was skipped (Figure 3D), resulting in the insertion of nine new amino acids followed by a premature stop codon at position 203. Moreover, the intensity ratio of the mutant compared to the normal band was increased by up to 67 % after treatment with 30  $\mu$ M cycloheximide, which inhibits NMD, compared to a ratio of 29 % in the untreated condition (Figure 3D, E). These facts suggest that the mutant mRNA possessing a premature stop codon suffered from degradation by NMD in neurons, resulting in haploinsufficiency.

Considering the degradation of STXBP1 proteins with missense mutations, NMD of mRNAs with premature stop codons and the effects of deletion of STXBP1, we conclude that haploinsufficiency of *STXBP1* causes OS.

## HOW WOULD HAPLOINSUFFICIENCY OF *STXBP1* LEAD TO OS?

### Impairment of Synaptic Vesicle Release

*STXBP1* (*MUNC18-1*) is a member of the evolutionarily conserved Sec1/Munc-18 gene family that acts at specific steps of intracellular membrane transport.<sup>26,27</sup> In mammalian exocytosis, the vesicular SNARE protein, VAMP2 (also known as *synaptobrevin2*), and the target

membrane SNARE proteins, Syntaxin-1 and SNAP25, constitute the core fusion machinery that bring two membranes into close apposition to fuse.<sup>22,28</sup> An *Stxbp1* null mutation led to complete loss of neurotransmitter secretion from synaptic vesicles throughout development in mice, though seizures have never been described.<sup>16</sup> Thus, *STXBP1* very likely plays a central role in synaptic vesicle release in coordination with SNARE proteins. The association of mutations of *STXBP1* with OS implies that perturbation of synaptic vesicle release forms part of the genetic basis of epilepsy. To date, the majority of genes associated with epilepsy syndromes are ion channel genes.<sup>29</sup> Synapsin I is a synaptic vesicle protein thought to regulate the kinetics of neurotransmitter release during priming of synaptic vesicles, and a mutation has been identified in a family with X-linked epilepsy and learning difficulties.<sup>30</sup> *STXBP1* is the second synaptic vesicle gene shown to be involved in epilepsy, and this finding will encourage further research into regulation of synaptic vesicle release and its involvement in seizures and related disorders.

### Possible Interneuropathy

In *Stxbp1* heterozygous knockout mice, no seizures have been reported, and whole-cell recordings of autaptic glutamatergic or GABAergic (GABA: gamma-aminobutyric acid) neurons showed excitatory and inhibitory postsynaptic currents similar to those of WT littermate neurons upon single depolarizations.<sup>31</sup> However, with repeated stimulation, *Stxbp1*<sup>+/-</sup> neurons showed impaired synaptic function due to the reduced size and replenishment rate of readily releasable vesicles,<sup>31</sup> suggesting that heterozygous deletion of *Stxbp1* indeed affected synaptic function in mice. Interestingly, the reduction of readily releasable vesicles was more evident in GABAergic neurons than in glutamatergic neurons.<sup>31</sup> It has been reported that *Arx* is expressed in GABAergic interneurons, and that *Arx* controls their genesis, migration, and differentiation, as *Arx*-knockout mice showed a deficit of GABAergic interneurons.<sup>32</sup> Moreover, neuropathological examination of three patients with X-linked lissencephaly with absent corpus callosum and ambiguous genitalia, caused by *ARX* mutations, has suggested a loss of interneurons.<sup>33</sup> If haploinsufficiency of *STXBP1* affected GABAergic interneurons more severely than glutamatergic neurons in humans as in mice, a defect in the GABAergic system could be postulated as a common pathophysiology among OS patients with *ARX* or *STXBP1* mutations. Ohtahara syndrome might be designated as a continuum of “interneuronopathies”.<sup>34,35</sup>

### Cell Death of the Brainstem

As brain malformations are often associated with individuals with OS,<sup>2,3</sup> it could be speculated that *STXBP1* mutations would lead to abnormal brain structures directly related to the seizure phenotype of OS. However, we did not observe structural brain anomalies in any of the 14 OS patients with *STXBP1* defects. This is consistent with the findings that mice deleted for *Stxbp1* have normal brain architecture. *Stxbp1* null mice, however, showed extensive cell death of mature neurons in lower brain areas, such as the brainstem; the lower brainstem was almost completely lost by embryonic day 18.<sup>16</sup> This is consistent with the suggestion that tonic seizures in OS might originate from subcortical structures, including the brainstem. Thus, in addition to the impaired synaptic vesicle release, it is possible that *STXBP1* haploinsufficiency leads to OS through microscopically impaired neuronal cell death in lower brain areas.

## FUTURE CHALLENGES

### Expansion of the Clinical Spectrum of *STXBP1* Mutations

Although OS is the core phenotype of *STXBP1* defects in our Japanese cohort (one third of OS cases harbored *STXBP1* mutations), Hamdan et al. recently reported that two *de novo* *STXBP1* mutations, c.1162C>T (p.R388X) and c.169+1G>A, were identified in 2 out of 95 individuals with MR and nonsyndromic epilepsy.<sup>36</sup> According to their report, the two patients

never showed the tonic seizures or infantile spasms associated with OS and WS, respectively. The onset of first seizures was at 6 weeks and 2 years of age, respectively. In addition, characteristic EEG patterns, such as suppression-burst or hypsarrhythmia, were never observed in these patients. Thus, the finding by Hamdan et al. indicated that *STXBP1* defects could cause a wide spectrum of clinical epileptic disorders in association with severe MR. Given that defects in synaptic dysfunction have also been implicated in many common neurodevelopmental disorders, such as MR, autism, and schizophrenia,<sup>37,38</sup> the possible involvement of *STXBP1* mutations in such common neurodevelopmental disorders is of interest. Elucidation of the molecular basis of synaptic vesicle processing disturbed by *STXBP1* mutations will allow us to understand not only the pathophysiology of infantile epilepsy, but also many neuropsychiatric conditions that present beyond childhood. The contribution of *STXBP1* mutations to EME also should be clarified, because myoclonic seizures, the characteristic feature of EME, are occasionally observed in 3/14 patients with *STXBP1* mutations.

### Animal Model

An animal model is necessary to elucidate the pathophysiology of epilepsy caused by *STXBP1* mutations, including age-dependency of seizure type and EEG pattern, and to test potential therapies directed specifically at OS and subsequent WS. The effect of gene dosage alterations of *STXBP1/Stxbp1* might vary between humans and mice: humans might be more susceptible than mice; thus, loss of function of one allele could cause seizures in humans but not in mice. Although it would be challenging to manipulate the gene dosage of *Stxbp1* - for example, in combination with a hypomorphic allele and a null allele - to the level at which mutant mice show a seizure phenotype, the establishment of an animal model will greatly benefit our understanding of the mechanisms of seizures in relation to impaired synaptic function.

### References

- Ohtahara S, Ishida T, Oka E, Yamatogi Y, Inoue H, Karita S, Ohtsuka Y. [On the specific age dependent epileptic syndrome: the early-infantile epileptic encephalopathy with suppression-burst.]. *No to Hattatsu* 1976;8:270–279.
- Djukic A, Lado FA, Shinnar S, Moshe SL. Are early myoclonic encephalopathy (EME) and the Ohtahara syndrome (EIEE) independent of each other? *Epilepsy Res* 2006;70(Suppl 1):S68–76. [PubMed: 16829044]
- Ohtahara S, Yamatogi Y. Ohtahara syndrome: with special reference to its developmental aspects for differentiating from early myoclonic encephalopathy. *Epilepsy Res* 2006;70(Suppl 1):S58–67. [PubMed: 16829045]
- Yamatogi Y, Ohtahara S. Early-infantile epileptic encephalopathy with suppression-bursts, Ohtahara syndrome; its overview referring to our 16 cases. *Brain Dev* 2002;24:13–23. [PubMed: 11751020]
- Kato M, Saitoh S, Kamei A, Shiraiishi H, Ueda Y, Akasaka M, Tohyama J, Akasaka N, Hayasaka K. A Longer Polyalanine Expansion Mutation in the ARX Gene Causes Early Infantile Epileptic Encephalopathy with Suppression-Burst Pattern (Ohtahara Syndrome). *Am J Hum Genet* 2007;81:361–366. [PubMed: 17668384]
- Fullston T, Brueton L, Willis T, Philip S, MacPherson L, Finnis M, Gecz J, Morton J. Ohtahara syndrome in a family with an ARX protein truncation mutation (c.81C>G/p.Y27X). *Eur J Hum Genet* 2010;18:157–162. [PubMed: 19738637]
- Absoud M, Parr JR, Halliday D, Pretorius P, Zaiwalla Z, Jayawant S. A novel ARX phenotype: rapid neurodegeneration with Ohtahara syndrome and a dyskinetic movement disorder. *Dev Med Child Neurol* 2009;3:305–307.
- Kato M, Koyama N, Ohta M, Miura K, Hayasaka K. Frameshift mutations of the ARX gene in familial Ohtahara syndrome. *Epilepsia* 2010;51:1679–1684. [PubMed: 20384723]
- Saitu H, Kato M, Mizuguchi T, Hamada K, Osaka H, Tohyama J, Uruno K, Kumada S, Nishiyama K, Nishimura A, Okada I, Yoshimura Y, Hirai S, Kumada T, Hayasaka K, Fukuda A, Ogata K,

- Matsumoto N. *De novo* mutations in the gene encoding STXBP1 (MUNC18-1) cause early infantile epileptic encephalopathy. *Nat Genet* 2008;40:782–788. [PubMed: 18469812]
10. Engel J Jr. Report of the ILAE classification core group. *Epilepsia* 2006;47:1558–1568. [PubMed: 16981873]
  11. Molinari F, Raas-Rothschild A, Rio M, Fiermonte G, Encha-Razavi F, Palmieri L, Palmieri F, Ben-Neriah Z, Kadhom N, Vekemans M, Attie-Bitach T, Munnich A, Rustin P, Colleaux L. Impaired mitochondrial glutamate transport in autosomal recessive neonatal myoclonic epilepsy. *Am J Hum Genet* 2005;76:334–339. [PubMed: 15592994]
  12. Molinari F, Kaminska A, Fiermonte G, Boddaert N, Raas-Rothschild A, Plouin P, Palmieri L, Brunelle F, Palmieri F, Dulac O, Munnich A, Colleaux L. Mutations in the mitochondrial glutamate carrier SLC25A22 in neonatal epileptic encephalopathy with suppression bursts. *Clin Genet* 2009;76:188–194. [PubMed: 19780765]
  13. Kato M, Das S, Petras K, Sawaishi Y, Dobyns WB. Polyalanine expansion of ARX associated with cryptogenic West syndrome. *Neurology* 2003;61:267–268. [PubMed: 12874418]
  14. Guerrini R, Moro F, Kato M, Barkovich AJ, Shiihara T, McShane MA, Hurst J, Loi M, Tohyama J, Norci V, Hayasaka K, Kang UJ, Das S, Dobyns WB. Expansion of the first PolyA tract of ARX causes infantile spasms and status dystonicus. *Neurology* 2007;69:427–433. [PubMed: 17664401]
  15. Stromme P, Mangelsdorf ME, Shaw MA, Lower KM, Lewis SM, Bruyere H, Lutcheraht V, Gedeon AK, Wallace RH, Scheffer IE, Turner G, Partington M, Frints SG, Fryns JP, Sutherland GR, Mulley JC, Gecz J. Mutations in the human ortholog of *Aristaless* cause X-linked mental retardation and epilepsy. *Nat Genet* 2002;30:441–445. [PubMed: 11889467]
  16. Verhage M, Maia AS, Plomp JJ, Brussaard AB, Heeroma JH, Vermeer H, Toonen RF, Hammer RE, van den Berg TK, Missler M, Geuze HJ, Sudhof TC. Synaptic assembly of the brain in the absence of neurotransmitter secretion. *Science* 2000;287:864–869. [PubMed: 10657302]
  17. Garcia EP, Gatti E, Butler M, Burton J, De Camilli P. A rat brain Sec1 homologue related to Rop and UNC18 interacts with syntaxin. *Proc Natl Acad Sci U S A* 1994;91:2003–2007. [PubMed: 8134339]
  18. Kalidas S, Santosh V, Shareef MM, Shankar SK, Christopher R, Shetty KT. Expression of p67 (Munc-18) in adult human brain and neuroectodermal tumors of human central nervous system. *Acta Neuropathol* 2000;99:191–198. [PubMed: 10672327]
  19. Saitsu H, Kato M, Okada I, Kenji O, Higuchi T, Hoshino H, Kubota M, Arai H, Kimura S, Sudo A, Miyama S, Takami Y, Watanabe T, Nishimura A, Nishiyama K, Miyake N, Wada T, Osaka H, Kondo N, Hayasaka K, Matsumoto N. *STXBP1* mutations in early infantile epileptic encephalopathy with suppression-burst pattern. *Epilepsia*. in press
  20. Kanazawa K, Kumada S, Kato M, Saitsu H, Kurihara E, Matsumoto N. Choreo-Ballistic Movements in a Case Carrying a Missense Mutation in Syntaxin Binding Protein 1. *Gene Mov Disord*. in press
  21. Dulubova I, Khvotchev M, Liu S, Huryeva I, Sudhof TC, Rizo J. Munc18-1 binds directly to the neuronal SNARE complex. *Proc Natl Acad Sci U S A* 2007;104:2697–2702. [PubMed: 17301226]
  22. Toonen RF, Verhage M. Munc18-1 in secretion: lonely Munc joins SNARE team and takes control. *Trends Neurosci* 2007;30:564–572. [PubMed: 17956762]
  23. Rickman C, Medine CN, Bergmann A, Duncan RR. Functionally and spatially distinct modes of munc18-syntaxin 1 interaction. *J Biol Chem* 2007;282:12097–12103. [PubMed: 17264080]
  24. Shyu AB, Wilkinson MF, van Hoof A. Messenger RNA regulation: to translate or to degrade. *EMBO J* 2008;27:471–481. [PubMed: 18256698]
  25. Maquat LE, Kinniburgh AJ, Rachmilewitz EA, Ross J. Unstable beta-globin mRNA in mRNA-deficient beta o thalassemia. *Cell* 1981;27:543–553. [PubMed: 6101206]
  26. Sudhof TC. The synaptic vesicle cycle. *Annu Rev Neurosci* 2004;27:509–547. [PubMed: 15217342]
  27. Weimer RM, Richmond JE. Synaptic vesicle docking: a putative role for the Munc18/Sec1 protein family. *Curr Top Dev Biol* 2005;65:83–113. [PubMed: 15642380]
  28. Rizo J, Rosenmund C. Synaptic vesicle fusion. *Nat Struct Mol Biol* 2008;15:665–674. [PubMed: 18618940]
  29. Gurnett CA, Hedera P. New Ideas in Epilepsy Genetics: Novel Epilepsy Genes, Copy Number Alterations, and Gene Regulation. *Arch Neurol* 2007;64:324–328. [PubMed: 17353374]